Multi Scale Modeling of Multi Phonon Hole Capture in the Context of NBTI

F. Schanovsky
CDL for Reliability Issues in Microelectronics
Institute for Microelectronics, TU Wien
Gußhausstraße 27-29/E360, 1040 Wien
Email: schanovsky@iue.tuwien.ac.at

O. Baumgartner and T. Grasser
Institute for Microelectronics, TU Wien
Gußhausstraße 27-29/E360, 1040 Wien
Fax: +43/1/58801-35099

***Abstract*—We report on a novel approach to the modeling of non-radiative multi phonon transitions in semiconductor devices. Using line shapes calculated from density functional theory, the hole capture rate due to a non-radiative multi phonon process is computed for an MOS structure. The charge carriers in the MOS structure are described using a non-equilibrium Green's function formalism that makes it possible to treat the device as an open quantum system. The dependence of the hole capture rate on the gate voltage and the temperature are calculated for the oxygen vacancy and the hydrogen bridge defect at different positions in the gate oxide.**

I. Introduction

One of the most pressing reliability issues today is the negative bias temperature instability (NBTI) [1], [2] in p-channel MOSFETs. It manifests itself as a degradation of the threshold voltage and the carrier mobility when a (large) negative bias is applied to the gate contact at elevated temperatures, while all other terminals are grounded.

Detailed experimental and theoretical investigations have shown that the physical origin of NBTI lies in the capture and emission of holes to and from defects in the isolating oxide of the MOS structure [3]. Recently, the analysis of small-area pMOSFETs, where the charge transitions of defects cause discrete steps in the NBTI recovery traces (see Fig. 1), has led to the development of the *time dependent defect spectroscopy* (TDDS) [4], [5], which has made it possible to study the detailed charging and discharging kinetics of the *defects* causing NBTI. TDDS has revealed very complex temperature activated and gate voltage dependent transition kinetics, which is explained using a newly developed defect model [5]. This model describes hole capture and release within the framework of non-radiative multi phonon (NMP) transitions [6], [7].

So far, the NMP transitions in the NBTI defect model are implemented in an approximate form [5], employing a number of parameters that are empirically adjusted to fit the experimental data. The present work reports a more sophisticated implementation of the NMP theory for oxide defects, combining state-of-the-art device modeling with a first-principles density functional theory (DFT) based description of the defect properties. It is meant as a proof-of-concept for extracting NMP properties for device modeling from DFT and also serves as a benchmark for computationally less expensive approximations.

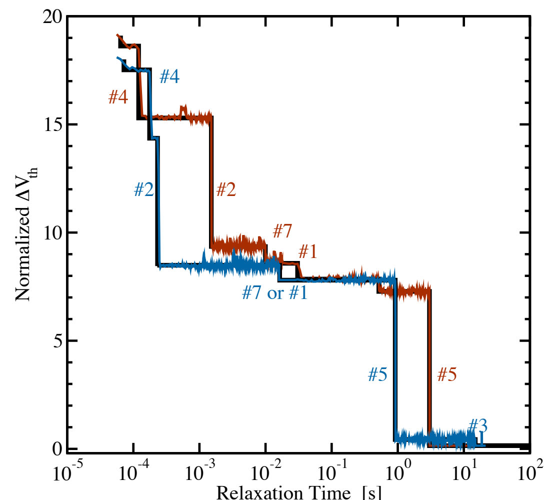

Fig. 1. In small-area pMOSFETs, NBTI recovery traces feature steps of varying size at different relaxation times. These steps have been attributed to the discharging of defects that have captured a hole during the stress phase. Using the TDDS method, the capture and emission kinetics of these defects can be studied [5].

II. NMP Transitions

Carrier transition processes involving multiple vibrational excitations of defects in semiconductors have been extensively studied in literature [6]–[9]. The rate k_{if} for a hole capture transition from the electronic state $|\Phi_\mathrm{i}\rangle$ to the state $|\Phi_\mathrm{f}\rangle$ is given by

$$k_{\mathrm{if}} = A_{\mathrm{if}} f \tag{1}$$

where

$$A_{\mathrm{if}} = \frac{2\pi}{\hbar} \left|\langle \Phi_\mathrm{f} | V' | \Phi_\mathrm{i} \rangle\right|^2 \tag{2}$$

and

$$f = \operatorname*{ave}_{\alpha} \sum_{\beta} \left|\langle \eta_{\mathrm{f}\beta} | \eta_{\mathrm{i}\alpha} \rangle\right|^2 \delta(E_{\mathrm{f}\beta} - E_{\mathrm{i}\alpha} + E). \tag{3}$$

f is called the line-shape function. It describes the dependence of the capture rate on the hole energy E and is an inherent property of the atomic structure of the defect. The line shape is

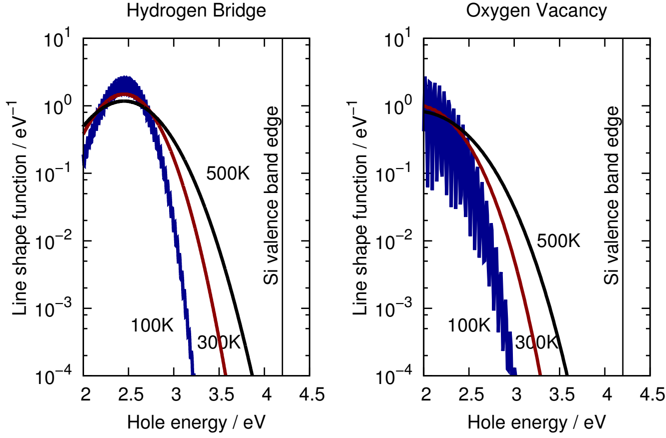

Fig. 2. The line shapes as calculated from DFT using Eq. 3 for three different temperatures. The 100K plots show oscillations as the quantum mechanical nature of the vibrational overlaps becomes more and more pronounced in this regime.

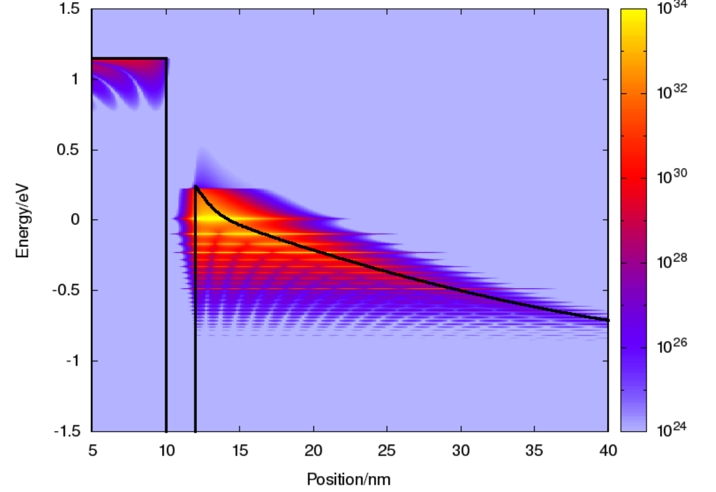

Fig. 3. The spatially and energetically distributed hole density as calculated using the NEGF method. Thermal equilibrium in the gate and the silicon bulk is induced via an optical potential. The penetration of holes into the oxide can be clearly seen.

determined by the overlaps of the vibrational wave functions associated with the initial and the final adiabatic potential energy surface $|\eta_{\mathrm{i}\alpha}\rangle$ and $|\eta_{\mathrm{f}\beta}\rangle$ as well as the respective energies $E_{\mathrm{f}\beta}$ and $E_{\mathrm{i}\alpha}$. We have recently devised a method to extract the line shape function from DFT defect calculations [10], [11]. In this method, approximate potential energy surfaces are extracted from DFT calculations as depicted in Fig. 4. These parabolic potential energy surfaces then determine harmonic oscillator vibrational wave functions that are used to construct line shapes via Eq. 3, using analytic expressions for the overlap integrals [12], [13]. The resulting line shapes consist of weighted Dirac peaks which are smeared by a normal distribution of standard deviation k_{B}. A more in-depth description of the line shape calculation can be found in [11], the results for the defects under consideration can be seen in Fig. 2.

Comparing with literature, the numerical calculation of line shapes from Franck-Condon overlap factors stands in contrast to implementations employing analytic formulae [14]–[16]. These formulae are not applicable in our case, as they are restricted to the assumption of linear electron phonon coupling, which is not fulfilled in our calculations.

A_{if} describes the electronic part of the transition. It contains the electronic matrix element between the initial and the final electronic state $|\Phi_{\mathrm{i}}\rangle$ and $|\Phi_{\mathrm{f}}\rangle$ via the perturbing potential V'. In an MOS device, none of these quantities is accurately known, and so this term has to be estimated [3], [7], [14]. In the present work, we approximate it as [17]

$$\left|\langle\Phi_{\mathrm{f}}|V'|\Phi_{\mathrm{i}}\rangle\right|^2 \approx \alpha\left|\langle x_{\mathrm{d}}|\phi_j\rangle\right|^2, \tag{4}$$

where x_{d} is the wave function of the hole to be captured.

In a semiconductor device, there is a reservoir of holes with different energies E_j, wave functions $|\phi_j\rangle$, associated occupation probabilities p_j, and multiplicities m_j. The total hole capture rate is found by summing up the contributions of all particles in the reservoir as

$$k_h \propto \sum_j p_j m_j \left|\langle x_{\mathrm{d}}|\phi_j\rangle\right|^2 f(E_j) \tag{5}$$

III. Non-Equilibrium Green's Functions

In the present work, the carrier concentration of the MOS structure has been calculated self-consistently using an open boundary non-equilibrium Green's function (NEGF) method [18]. The formalism assumes thermal equilibrium in the gate and bulk region where level broadening due to scattering is modeled using an optical potential. The oxide is treated as a non-equilibrium domain with ballistic quantum transport.

Due to the open boundary conditions, there are no sharp eigenstates for the hole wave functions. Instead, there is a nonzero probability to find a hole at every energy level. From the Green's function, the local density of states

$$D(x,E) = m(E)\left|\langle x|\phi(E)\rangle\right|^2 \delta(E) \tag{6}$$

as well as the occupation probability $p(x,E)$ can be computed, an example is shown in Fig. 3. To obtain the total NMP hole capture rate k_h for a defect at position x_{d}, one just has to insert these quantities into Eq. 5 and replace the sum by an integral to obtain

$$k_h = \alpha \int f(E) h(x_{\mathrm{d}}, E) dE \text{ where} \tag{7}$$

$$h(E) = p(E) D(E). \tag{8}$$

The remaining unknown is the factor α, which is eliminated in this work by scaling all capture rates and time constants by defined values. The integration is implemented as a post-processing step using the numerical NEGF and line shape data.

One advantage of the NEGF approach is the absence of any artificial boundaries within the device, e.g. a Dirichlet boundary condition at the semiconductor-oxide-interface as

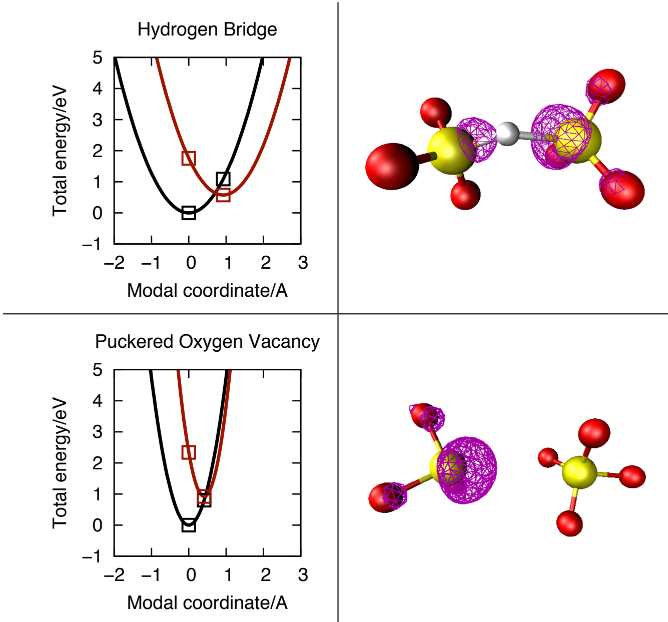

Fig. 4. To extract line shapes from DFT calculations, approximate parabolic potential energy surfaces are extracted (left) for the defect in its neutral (black) and positive (red/gray) configuration. The square symbols indicate the points calculated using DFT [10]. The atomic defect models are illustrated on the right. The partial charge densities associated with the defect are shown as wire frame.

usually employed in closed-boundary MOS device calculations [14], [15]. Also, it allows the injection of holes from the gate to be taken into consideration.

IV. Calculation details

The electronic structure of the defect is described with DFT using the PBE functional [19], [20]. The atomistic host lattice is an orthorhombic alpha-quartz supercell structure [10], [21] containing 72 atoms. Alpha Quartz was chosen because it is a well studied reference system for amorphous silica [21]–[23]. The defect energies are aligned to the hole reservoir using the valence level of the DFT reference system [24], as the energy levels of the investigated defects are in the lower half of the SiO_2 band gap. More details on the DFT part can be found elsewhere [10], [11], [17].

The MOS structure consists of a poly-Si gate and an n-doped bulk separated by a 2nm SiO_2 layer. For electrons the unprimed and primed valleys with $0.19\mathrm{m_e}$ and $0.91\mathrm{m_e}$ electron mass are included. Holes were considered with $0.49\mathrm{m_e}$ effective mass.

The calculation of the NMP hole capture rates proceeds in a two-step process. At first, the band bending is calculated by solving the Poisson- and the NEGF equations self-consistently. Secondly, the NEGF problem is again solved non-self-consistently on a different energy grid that accounts for high-energy holes as these contribute considerably to the NMP transitions.

For the evaluation of the integral Eq. 7, it is necessary to align the energy scales of the DFT defect model and the NEGF device model. In the present work we chose the SiO_2 valence band edge, which was also taken as the reference energy in the DFT calculations, as the common alignment energy. For oxide defects, the dependence of the line shape on the value of the reference energy at the defect site plays a crucial role for the transition kinetics, as the band bending energetically shifts the line shape, leading to large changes in the capture rate.

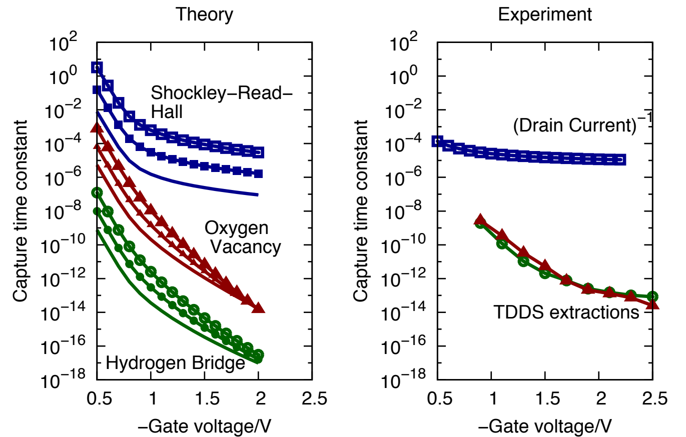

Fig. 5. Gate voltage dependence of the hole capture time constant. All time constants are normalized. In the left figure, the results for the hydrogen bridge and for the oxygen vacancy are compared to a Shockley-Read-Hall like capture model, which shows much weaker gate voltage dependence in deep inversion. The calculation temperature is 400K and the defect position is 2 (no symbols), 4 (medium sized symbols) and 6 (large symbols) angstroms from the silicon bulk. The right figure shows the experimental situation. Capture time constants extracted using the TDDS technique [5] are compared with the inverse of the drain current, which is proportional to what would be seen for Shockley-Read-Hall-like defects.

V. Results

Fig. 5 left shows the gate voltage dependence of the NMP hole capture time constants for the two model defects. For comparison, a Shockley-Read-Hall [25] (SRH) capture time constant is shown. The SRH model assumes that the capture rate is proportional to the total hole density at the defect site. The NMP defects clearly show a much stronger gate voltage dependence than the SRH defect. Further, the gate voltage dependence increases with the distance of the defect from the silicon bulk. Both of these strong dependencies are caused primarily by the energetic shift of the line shape functions relative to the holes in the inversion layer. This shift in turn arises from the different band bending at different applied voltages. Comparing Fig. 5 right shows that the NMP defects are consistent with the qualitative behavior of defects observed in TDDS measurements.

The temperature dependence of the hole capture is shown in Fig. 6. The calculation of NMP hole capture rates for the given defects becomes technically challenging for low temperatures. As the temperature decreases, the line shapes become increasingly narrow, thus making high-energy holes the dominantly captured particles. Accurate representation of high-energy holes in the NEGF algorithm requires an improved refinement strategy for the energy grid. To overcome

this limitation, the hole distribution over energy was calculated from a classical density of states for the Arrhenius plot, taking only the total hole concentration at the defect site from the NEGF calculation.

NMP defects show a strong temperature activation, in good agreement with experimental observation and in contrast to the SRH description. Also, the difference between line shapes calculated using the quantum mechanical formula of Eq. 3 and those calculated based on classical statistical physics are compared. For the hydrogen bridge, this difference becomes visible below 140K. For the oxygen vacancy, the classical formula reproduces the quantum mechanical behavior over the complete temperature range investigated.

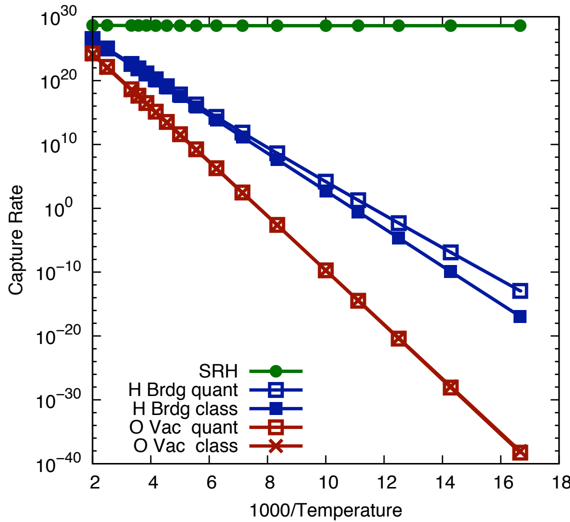

Fig. 6. Arrhenius plots of the capture rates for the defect types comparing the quantum mechanical NMP capture rates Eq. 3 for the oxygen vacancy and the hydrogen bridge to the capture rates calculated using classical point-like atoms and to a Shockley-Read-Hall like model.

VI. Conclusion

We report a detailed model to describe non-radiative multi phonon hole capture during NBTI degradation. Our approach combines a density functional theory for the defect and a non-equilibrium Green's function model for the device to obtain an accurate description of the real-world situation. The implementation of the non-radiative multi phonon transitions deviates from published implementations by employing numerically calculated line shapes instead of analytic expressions.

The calculations have been compared to experimental data obtained using the time-dependent defect spectroscopy on small-area MOSFETs. The gate voltage dependence of the calculated capture time constants show good qualitative agreement with experiment. Also, the reported strong temperature activation can be explained by the NMP model. Line shapes calculated from classical statistical physics have been compared to their fully quantum mechanical counterparts. The classical approximation is shown to give a good approximation for the considered defects for the temperatures typically encountered during device operation.

References

[1] K. O. Jeppson and C. M. Svensson, "Negative bias stress of MOS devices at high electric fields and degradation of MNOS devices," *J.Appl.Phys.*, vol. 48, no. 5, pp. 2004–2014, 1976.

[2] D. K. Schroder, "Negative bias temperature instability: What do we understand?" *Microelectronics Reliability*, vol. 47, pp. 841–852, 2007.

[3] T. Grasser *et al.*, "A Two-Stage Model for Negative Bias Temperature Instability," in *Proc. Intl.Rel.Phys.Symp.*, 2009, pp. 33–44.

[4] ——, "Time-Dependent Defect Spectroscopy for Characterization of Border Traps in Metal-Oxide-Semiconductor Transistors," *Physical Review B*, vol. 82, pp. 245 318–1, 2010.

[5] ——, "The Time Dependent Defect Spectroscopy (TDDS) Technique for the Characterization of the Bias Temperature Instability," in *Proc. Intl.Rel.Phys.Symp.*, 2010, pp. 16–25.

[6] C. H. Henry and D. V. Lang, "Nonradiative capture and recombination by multiphono emission in GaAs and GaP," *Physical Review B*, vol. 15, no. 15, pp. 989–1016, January 1977.

[7] S. Makram-Ebeid and M. Lannoo, "Quantum model for phonon-assisted tunnel ionization of deep levels in a semiconductor," *Physical Review B*, vol. 25, no. 10, pp. 6406–6424, May 1982.

[8] A. Schenk, "An improved approach to the Shockley-Read-Hall recombination in inhomogeneous fields of space-charge regions," *J.Appl.Phys.*, vol. 71, pp. 3339–3349, 1992.

[9] K. Huang and A. Rhys, "Theory of light absorption and non-radiative transitions in F-centers," *Proc. Roy. Soc. A*, vol. 204, pp. 406–423, 1950.

[10] F. Schanovsky, W. Goes, and T. Grasser, "An Advanced Description of Oxide Traps in MOS Transistors and its Relation to DFT," *J.Comp.Elect.*, vol. 9, pp. 135–140, 2010.

[11] ——, "Multi-phonon hole-trapping from first principles," *J.Vac.Sci.Technol.B*, vol. 29, pp. 01A201–1, 2011.

[12] B. Zapol, "New expressions for the overlap integral of two linear harmonic oscillator wavefunctions," *Chem.Phys.Lett.*, vol. 93, no. 6, pp. 549–552, 1982.

[13] P. P. Schmidt, "Computationally efficient recurrence relations for one-dimensional Franck-Condon overlap integrals," *Molecular Physics*, vol. 108, pp. 1513–1529, 2010.

[14] A. Palma *et al.*, "Quantum two-dimensional calculation of time constants of random telegraph signals in metal-oxide-semiconductor structures," *Physical Review B*, vol. 56, no. 15, pp. 9565–9574, October 1997.

[15] D. Garetto *et al.*, "Small signal analysis of electrically-stressed oxides with Poisson-Schroedinger based multiphonon capture model," in *Proc. Intl.Workshop on Comput. Electron.*, 2010.

[16] J. H. Zheng, H. S. Tan, and S. C. Ng, "Theory of non-radiative capture of carriers by multiphonon processes for deep centers in semiconductors," *J.Phys.:Condensed Matter*, vol. 6, pp. 1695–1706, 1994.

[17] F. Schanovsky, "Ab-Initio Calculation of the Vibrational Influence on Hole-Trapping," in *Proc. Intl.Workshop on Comput. Electron.*, 2010.

[18] O. Baumgartner, M. Karner, and H. Kosina, "Modeling of high-k-Metal-Gate-stacks using the non-equilibrium Green's function formalism," in *Proc. Simulation of Semiconductor Processes and Devices*, 2008, pp. 353 –356.

[19] G. Kresse and J. Furthmüller, "Efficient iterative schemes for ab initio total-energy calculations using a plane-wave basis set," *Physical Review B*, vol. 54, no. 11, pp. 11 169–11 186, 1996.

[20] G. Kresse and D. Joubert, "From ultrasoft pseudopotentials to the projector augmented-wave method," *Physical Review B*, vol. 59, p. 1758, 1999.

[21] P. E. Blöchl, "First-principles calculations of defects in oxygen-deficient silica exposed to hydrogen," *Physical Review B*, vol. 62, no. 10, pp. 6158–6178, September 2000.

[22] J. K. Rudra and W. B. Fowler, "Oxygen vacancy and the E'_1 center in crystalline SiO_2," *Physical Review B*, vol. 35, no. 15, pp. 8223–8230, 1987.

[23] A. S. Mysovsky *et al.*, "Calibration of embedded-cluster method for defect studies in amorphous silica," *Physical Review B*, vol. 69, no. 8, p. 085202, 2004.

[24] D. A. Drabold and S. K. Estreicher, Eds., *Theory of Defects in Semiconductors*. Springer, 2010.

[25] W. Shockley and W. T. Read, "Statistics of the Recombinations of Holes and Electrons," *Physical Review*, vol. 87, pp. 835–842, 1952.